

AUTOMATIC CAR STEERING CONTROL BRIDGES OVER THE DRIVER REACTION TIME

JÜRGEN ACKERMANN AND TILMAN BÜNTE

A car driver needs at least five hundred milliseconds before he can react to unexpected yaw motions. During this time the uncontrolled car may produce a dangerous yaw rate and sideslip angle. Automatic steering control for disturbance rejection is designed such that it bridges over the driver reaction time, but returns the full steering authority to the driver thereafter. The solution is robust with respect to uncertainties in the road-tire contact and in the mass and velocity of the vehicle. The yaw disturbance transfer function is compared with those of the ideally decoupled car and of the uncontrolled car. The frequency responses are evaluated in the form of disturbance attenuation ratios and frequency limits.

1. INTRODUCTION

Critical car driving situations arise, when a disturbance torque acts on the vehicle. Examples are crosswind, flat tire, braking on a slippery road and gas release in a curve. It takes the driver at least five hundred milliseconds to react to the resulting yaw motion of his car. During this time the tire sideforce may already reach its physical limits. A delayed overreaction of the driver may also cause driver-induced oscillations. Such dangerous situations can be avoided by robust decoupling of car steering [1, 2]. On the other hand, the driver should not be cheated by the feedback control system. In particular he should feel a similar response to his steering commands as in the uncontrolled car. This applies both to the immediate reaction after a step input at the steering wheel and to the required steering-wheel angle for steady-state cornering. These requirements call for a modification of the decoupling control law.

In Section 2 of this paper the model for the car steering dynamics is introduced. In Section 3 the properties of the robust decoupling control law are analyzed. Section 4 introduces the modified control law. Some simulation results are shown in Section 5 to compare the conventional car with both controlled cars. In Section 6 another way of comparison is performed in the frequency domain. Yaw disturbance attenuation ratios of the controlled cars with respect to the conventional car are determined.

2. CAR STEERING DYNAMICS

Consider the vehicle of Figure 1. Vehicle data are usually given in the form of l_r, l_f , vehicle mass m , and moment of inertia J w.r.t. a vertical axis through the CG. These quantities are related with the quantities m_1, m_r, l_1 of Figure 1 by

$$m = m_1 + m_r \quad (1)$$

$$J = m_1 l_1^2 + m_r l_r^2 \quad (2)$$

$$m_1 l_1 = m_r l_r. \quad (3)$$

(2) may be expressed using (3) as

$$J = m_r l_r l_1 + m_1 l_r l_1$$

and with (1)

$$J = m l_r l_1. \quad (4)$$

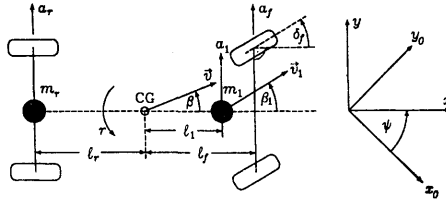


Fig. 1. Vehicle with arbitrary mass distribution.

The resulting length is

$$l_1 = \frac{J}{m l_r}.$$

There is a one-to-one relationship between the parameter sets (m, J, l_r, l_f) and (m, l_1, l_r, l_f) . We will use l_1 in the derivation of the model. The mass m is considered as a constant but uncertain parameter, $m \in [m^-; m^+]$. The corresponding moment of inertia follows from (4). Input to the system is the front-wheel steering angle δ_f , output is the yaw rate $r = \dot{\psi}$ measured by a gyro. For small steering angle δ_f and small sideslip angle β the standard single-track model of car steering [3] is

$$\begin{bmatrix} m v (\beta + r) \\ J \dot{r} \end{bmatrix} = \begin{bmatrix} F_y \\ M_z \end{bmatrix} + \begin{bmatrix} 0 \\ M_d \end{bmatrix}. \quad (5)$$

Only a disturbance torque M_d is assumed and no disturbance lateral force, because the latter is easily compensated by the driver in the course of his normal steering. The velocity v is a further constant but uncertain parameter, $v \in [v^-; v^+]$.

The steering force F_y and torque M_z are generated by the lateral tire forces $F_f(\alpha_f)$ and $F_r(\alpha_r)$ via

$$\begin{bmatrix} F_y \\ M_z \end{bmatrix} = \begin{bmatrix} 1 & 1 \\ l_f & -l_r \end{bmatrix} \begin{bmatrix} F_f(\alpha_f) \\ F_r(\alpha_r) \end{bmatrix}. \quad (6)$$

The tire forces depend on the tire sideslip angles α_f and α_r as illustrated in Figure 2 for the front wheel.

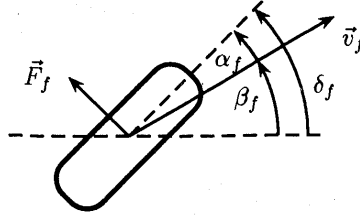


Fig. 2. Variables of the tire model.

The sideslip angle at the front mass β_1 will be introduced as a state variable. The sideslip angles at the CG (β) and at the axles (β_r, β_f) are related with β_1 by the kinematic relations for small angles

$$\begin{aligned}\beta &= \beta_1 - \frac{\ell_1}{v} r \\ \beta_f &= \beta_1 + \frac{\ell_f - \ell_1}{v} r \\ \beta_r &= \beta_1 - \frac{\ell_1 + \ell_r}{v} r.\end{aligned}\quad (7)$$

The local velocity vector \vec{v}_f forms the (chassis) slip angle β_f with the car body and the tire slip angle α_f with the tire direction, thus

$$\alpha_f = \delta_f - \beta_f = \delta_f - \beta_1 - \frac{\ell_f - \ell_1}{v} r. \quad (8)$$

In this paper we do not use rear wheel steering, i. e. $\delta_r \equiv 0$.

$$\alpha_r = \delta_r - \beta_r = -\beta_1 + \frac{\ell_1 + \ell_r}{v} r. \quad (9)$$

The tire force characteristics are linearized as

$$\begin{aligned}F_f(\alpha_f) &= c_f \alpha_f \\ F_r(\alpha_r) &= c_r \alpha_r\end{aligned}\quad (10)$$

where the cornering stiffnesses c_f and c_r are uncertain parameters that vary with the road tire contact. We assume $c_f = \mu c_{f0}$, $c_r = \mu c_{r0}$ where c_{f0} and c_{r0} are nominal values for the dry road and $\mu \in [\mu^-; 1]$ is an uncertain parameter ($\mu^- > 0$). The model (5), (6) with the above equations substituted becomes

$$\begin{bmatrix} mv(\beta_1 - \frac{\ell_1}{v} \dot{r} + r) \\ m\ell_r \dot{\ell}_1 \dot{r} \end{bmatrix} = \begin{bmatrix} 1 & 1 \\ \ell_f & -\ell_r \end{bmatrix} \begin{bmatrix} c_f(\delta_f - \beta_1 - \frac{\ell_f - \ell_1}{v} r) \\ c_r(-\beta_1 + \frac{\ell_1 + \ell_r}{v} r) \end{bmatrix} + \begin{bmatrix} 0 \\ M_d \end{bmatrix}$$

and, solving for $\dot{\beta}_1$ and \dot{r} ,

$$\begin{bmatrix} \dot{\beta}_1 \\ \dot{r} \end{bmatrix} = \begin{bmatrix} \frac{\ell_f + \ell_r}{m\ell_r v} & 0 \\ \frac{\ell_f}{m\ell_1 \ell_r} & -\frac{1}{m\ell_1} \end{bmatrix} \begin{bmatrix} c_f(\delta_f - \beta_1 - \frac{\ell_f - \ell_1}{v} r) \\ c_r(-\beta_1 + \frac{\ell_1 + \ell_r}{v} r) \end{bmatrix} - \begin{bmatrix} 1 \\ 0 \end{bmatrix} r + \begin{bmatrix} \frac{1}{m\ell_r v} \\ \frac{1}{m\ell_1 \ell_r} \end{bmatrix} M_d.$$

This form shows that $\dot{\beta}_1$ does not depend directly on the forces at the rear tires. An indirect coupling occurs through the r -terms in the equation for $\dot{\beta}_1$. These r -terms will be cancelled by the decoupling control law in order to make r unobservable from β_1 and from the lateral acceleration a_1 of the front mass m_1 . The state equations of the system are

$$\begin{bmatrix} \dot{\beta}_1 \\ \dot{r} \end{bmatrix} = \begin{bmatrix} c_1 & c_2 \\ c_3 & c_4 \end{bmatrix} \begin{bmatrix} \beta_1 \\ r \end{bmatrix} + \begin{bmatrix} \frac{c_f(\ell_f + \ell_r)}{m\ell_r v} \\ \frac{c_f \ell_f}{m\ell_1 \ell_r} \end{bmatrix} \delta_f + \begin{bmatrix} \frac{1}{m\ell_r v} \\ \frac{1}{m\ell_1 \ell_r} \end{bmatrix} M_d \quad (11)$$

$$\begin{aligned} c_1 &= -\frac{c_f(\ell_f + \ell_r)}{m\ell_r v} \\ c_2 &= -1 - \frac{c_f(\ell_f + \ell_r)(\ell_f - \ell_1)}{m\ell_r v^2} \\ c_3 &= \frac{(c_r \ell_r - c_f \ell_f)}{m\ell_1 \ell_r} \\ c_4 &= -\frac{\ell_1(c_f \ell_f - c_r \ell_r) - c_f \ell_f^2 - c_r \ell_r^2}{m\ell_1 \ell_r v} \end{aligned}$$

For the *conventional car* the front steering angle δ_f is generated by the steering wheel angle δ_L via the steering gear.

$$\delta_f(s) = \frac{\delta_L(s)}{i_L}, \quad (12)$$

i_L denotes the transmission ratio of the steering gear.

Consider now the lateral acceleration a_1 at the front mass m_1 , see Figure 1. It is related with the model quantities by

$$a_1 = a_{CG} + \ell_1 \dot{r} = \frac{F_f(\alpha_f) + F_r(\alpha_r)}{m} + \ell_1 \dot{r}. \quad (13)$$

Thus the steering transfer function from $\delta_L(s)$ to $a_1(s)$ (to be solved from (8), (9), (10), (11), (12) and (13)) reads

$$\begin{aligned} a_1(s) &= \frac{p_0 + p_1 s + p_2 s^2}{q_0 + q_1 s + q_2 s^2} \frac{\delta_L(s)}{i_L} \quad (14) \\ p_0 &= c_f c_r (\ell_f + \ell_r) v^2 \\ p_1 &= c_f c_r (\ell_f + \ell_r) (\ell_1 + \ell_r) v \\ p_2 &= c_f (\ell_f + \ell_r) \ell_1 m v^2 \\ q_0 &= c_f c_r (\ell_f + \ell_r)^2 + (c_r \ell_r - c_f \ell_f) m v^2 \\ q_1 &= (c_r \ell_r (\ell_r + \ell_1) + c_f (\ell_f^2 + \ell_r \ell_1)) m v \\ q_2 &= \ell_1 \ell_r m^2 v^2. \end{aligned}$$

3. ROBUST DECOUPLING CONTROL LAW

Robust decoupling [1] is achieved by the feedback control law

$$\delta_f(s) = \frac{1}{s} \left[K_L(v) \frac{\delta_L(s)}{i_L} - r(s) + \frac{\ell_f - \ell_1}{v} s r(s) \right]. \quad (15)$$

$K_L(v)$ is the steady-state yaw rate response to a unit step input for a nominal model ($\mu = \mu_0$ and $m = m_0$). It can be computed by (11) with $\beta_1 = \dot{r} = M_d = 0$ and $\delta_f = 1$.

$$K_L(v) = \frac{v}{(\ell_f + \ell_r) \left(1 + \frac{v^2}{v_{CH}^2} \right)} \quad (16)$$

$$v_{CH}^2 = \frac{c_{f0} c_{r0} (\ell_f + \ell_r)^2 \mu_0}{(c_{r0} \ell_r - c_{f0} \ell_f) m_0}.$$

A possible implementation is to measure the velocity v and to use it for gain-scheduling of $K_L(v)$.

The properties of the decoupling control law are

- The coupling from the yaw mode into the lateral acceleration a_1 has been removed. Thereby the steering transfer function from $\delta_L(s)$ to $a_1(s)$ is of first order ($M_d(s) \equiv 0$).

$$a_1(s) = \frac{v K_L(v)}{1 + \frac{\ell_r m v}{c_f (\ell_f + \ell_r)} s} \frac{\delta_L(s)}{i_L}. \quad (17)$$

The influence of the uncertain parameters m, v and μ has been drastically reduced by decoupling. Theoretically the steering dynamics can be made arbitrarily fast by additional high-gain feedback of a_1 , measured by an accelerometer, to δ_L . There are practical gain limitations, however, due to the measurement noise of the accelerometers and unmodelled higher-frequency dynamics that increase the phase of (17) beyond 180° . The task of the driver is only to keep the point mass m_1 on top of his planned path by commanding a_1 . He does not have to care about the stable yaw motion [1].

- For a step input of the yaw disturbance M_d (e.g. from crosswind, μ -split braking) the *conventional car* has a nonzero steady state value of the yaw rate, whereas for the *decoupled car* the yaw rate quickly returns to zero [2] as will be shown in section 6. Important safety advantages have been demonstrated in crosswind und μ -split braking with a test car [4].

On the other hand, the decoupling control law (15) also has some disadvantages that motivate the modifications in the next section.

- By the integration in the control law there is no immediate reaction of a_1 after a step command at δ_L . The driver feels that the car is not reacting as

promptly as the *conventional car*. Therefore a direct throughput from δ_L to δ_f will be provided, i. e. $\delta_f = \delta_L/i_L + \delta_c$, where δ_L/i_L is the steering angle as in the *conventional car*, and δ_c is an additional steering angle produced by the controller (15). This change does not affect the feedback path from r to δ_f and consequently the decoupling and the disturbance attenuation properties of the control law (15) are preserved.

- For safety reasons δ_c should be limited. Then the integrator must be unloaded in order to prevent its saturation.
- The yaw damping is decreased at high velocity. In [2] a good yaw damping was achieved by rear-wheel steering, which is not available under the assumptions of this paper. Another remedy is a velocity scheduled feedback of the lateral rear axle acceleration a_r to δ_c [5]. Then for low and medium velocities the robust decoupling is exact, but at high velocity a tradeoff between decoupling and yaw damping is made. A third idea is introduced in this paper. The main idea is to provide the decoupling action only for the first 0.5 seconds after a step input and thereafter to return smoothly to the properties of the *conventional car*, i. e. δ_c should follow the integral action only initially and then return to zero. Regarding a disturbance step M_d this concept helps the driver during the first half second by providing an additional steering angle much faster than the driver can react. Thereafter it returns the full authority gradually back to the driver. Reasonable yaw damping can be achieved by tuning the parameters of the filter which is employed to implement the fading decoupling action.
- The feedback from r provides an additional term to δ_f . In steady-state cornering there is no need for this term, the controlled car should behave like the *conventional car* in this situation, i. e. the driver should apply the same δ_L . The above modification takes care of this requirement.

4. THE MODIFIED CONTROL LAW

The modified control law is

$$\begin{aligned}\delta_f(s) &= \frac{\delta_L(s)}{i_L} + \delta_c(s) \\ \delta_c(s) &= \frac{s}{s^2 + 2D\omega_0 s + \omega_0^2} x_1(s) \\ x_1(s) &= K_L(v) \frac{\delta_L(s)}{i_L} - r(s) + \frac{\ell_f - \ell_1}{v} s r(s).\end{aligned}\tag{18}$$

Now there is a direct throughput of the input by the steering wheel δ_L to the front wheel steering angle δ_f . The pure integrator in (15) has been replaced by a dynamical filter ("fading integrator"). The initial behaviour ($s \rightarrow \infty$) of this filter to any input is the same as the response of an integrator. But the steady-state output of the filter ($s \rightarrow 0$) is zero. In the meantime the filter is unloaded so that after some time

the responsibility is softly returned to the driver. In steady-state cornering the car controlled by (18) (*car with fading integrator*) behaves like the *conventional car*.

Hence by the modified control law both the immediate and the long term reaction to any driver input is the same for the controlled car as for the uncontrolled car. But the transient behaviour is different as well as the disturbance rejection property of both systems.

5. SIMULATION RESULTS

In the following simulation study we use the data of a BMW 735i passenger car. They are

$$\begin{aligned} \ell_1 &= \ell_f = 1.514 \text{ m} \\ \ell_r &= 1.323 \text{ m} \\ m &= 1916 \text{ kg} \\ c_{f0} &= 49400 \text{ N/rad} \\ c_{r0} &= 103800 \text{ N/rad.} \end{aligned}$$

Concerning the *fading integrator*, the values of filter bandwidth ω_0 and filter damping coefficient D can be set in the controller design for a specific car.

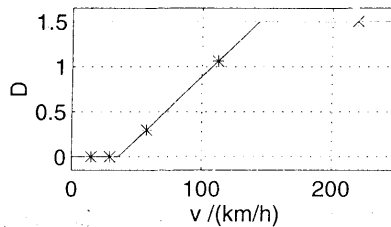


Fig. 3. $D(v)$.

We choose a filter bandwidth $\omega_0 = 1/\text{sec}$ to provide the above described properties (the decoupling action is supposed to fade out after ca. 0.5 seconds). The damping of the filter is tuned by the value of D . It turned out, that a scheduling of this parameter by velocity is useful to achieve a reasonable damping at all velocities. In simulations a table-lookup as shown in Figure 3 was found as a good function $D(v)$.

Three versions of the car are compared in the following simulation plots of the yaw rate r and additional steering angle δ_c .

1. The *conventional car*. Equation (11) is employed to compute the yaw rate response to yaw disturbance torque step inputs or steering wheel step inputs respectively. The "control law" is just $\delta_f(s) = \delta_L(s)/i_L$. The additional steering angle is zero. Dash-dotted line style is used for the time response plots and circles denote the eigenvalue position in the s -plane.

2. The *decoupled car* with direct throughput. To obtain comparable results with the two other versions of the car, the direct throughput is combined with the robust decoupling control law (15). Thus the steering angle equation reads

$$\delta_f(s) = \frac{\delta_L(s)}{i_L} + \frac{1}{s} \left[K_L(v) \frac{\delta_L(s)}{i_L} - r(s) + \frac{\ell_f - \ell_1}{v} s r(s) \right]. \quad (19)$$

Dashed line style for the responses and star markers for the eigenvalues are employed.

3. The *car with fading integrator*. The steering angle equation is (18). Plots use solid line style for the responses and x-marks for the eigenvalues.

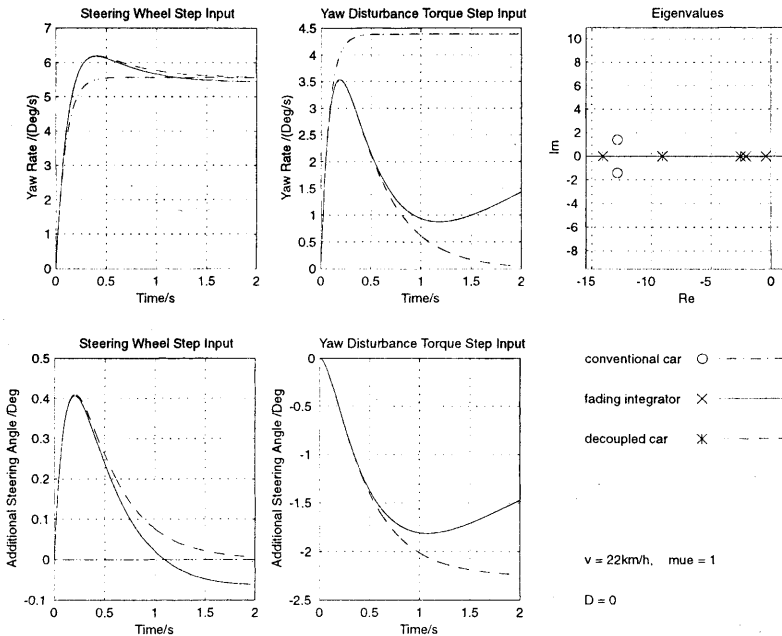


Fig. 4. Response to steering wheel step and yaw disturbance torque step for $v = 22 \text{ km/h}$.

In the first simulation of Figure 4 a steering wheel step input is applied to the three cars at a low speed of $v = 22 \text{ km/h}$. There is not much difference between the three versions. Both the *decoupled car* and the *car with fading integrator* perform a little overshoot in the yaw rate. With the simulation in Figure 4 for a disturbance torque step input the concept of fading out the decoupling action is well recognizable. Within the first 0.5 seconds both the *decoupled car* and the *car with fading integrator* provide the same disturbance rejection activity. However after 0.5 seconds for the *car with fading integrator* the steering authority is softly returned to the driver and

the additional steering angle δ_c goes to zero. For the driver it is early enough to react after one second to the yaw disturbance. The right upper plot of Figure 4 shows the eigenvalues for $v = 22$ km/h. They are well damped for all three versions.

Figure 5 shows the responses at a high speed of $v = 180$ km/h. The yaw damping for all versions is worse than at lower speeds. The worst damping occurs for the *decoupled car*. The oscillations of the *car with fading integrator* after a steering wheel step input decrease as quickly as those of the *conventional car* although the damping of the corresponding eigenvalues is less but their natural frequency is higher. The yaw disturbance responses show again how the initial decoupling action is fading out.

Figure 6 shows the result of deviations of the real car from the nominal model (used for the feedforward gain $K_L(v)$ in (16)) by reduction of the road adhesion factor to $\mu = 0.5$ at a medium velocity of $v = 72$ km/h. The steady-state responses of the *car with fading integrator* are the same as for the *conventional car*, whereas the *decoupled car* has a nonzero steady-state value of the additional steering angle.

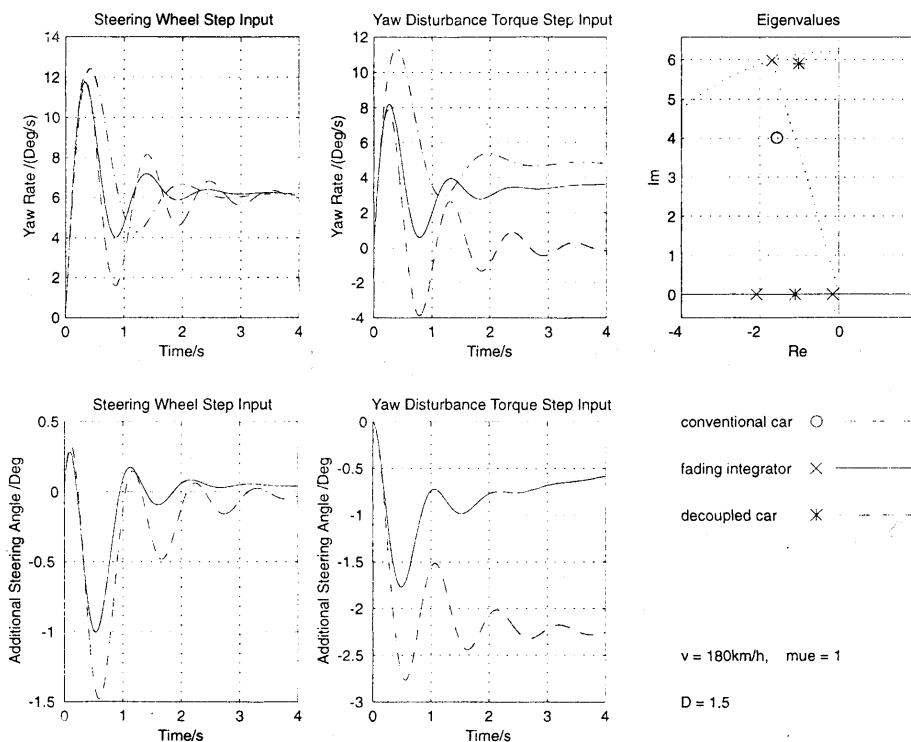


Fig. 5. Response to steering wheel step and yaw disturbance torque step for $v = 180$ km/h.

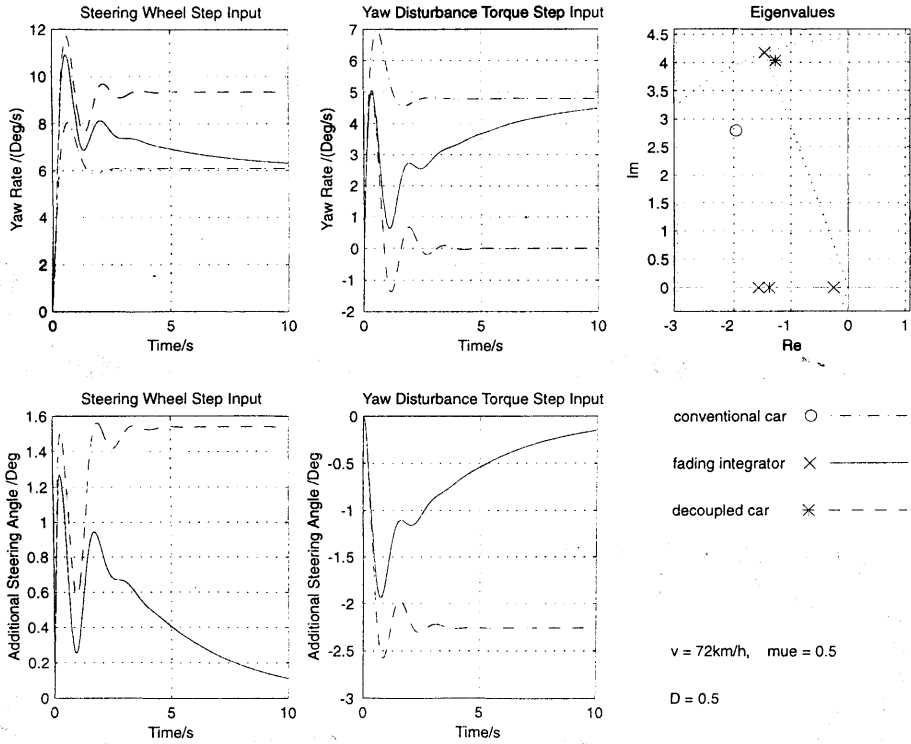


Fig. 6. Response to steering wheel step and yaw disturbance torque step for $\mu = 0.5$ at $v = 72$ km/h.

6. DISTURBANCE ATTENUATION PROPERTIES OF THE ROBUST DECOUPLING LAW AND THE MODIFIED CONTROL LAW

In this section, the disturbance attenuation of the closed control loop is analyzed in the frequency domain. The steering wheel angle is $\delta_L(s) \equiv 0$.

For the *conventional car* solve (11) for $\beta_1(s)$ and $r(s)$ and let $\delta_f(s) \equiv 0$.

$$\begin{bmatrix} \beta_1(s) \\ r(s) \end{bmatrix} = \frac{1}{D(s)} \begin{bmatrix} B(s) \\ R(s) \end{bmatrix} m_d(s) \quad (20)$$

$$B(s) = l_1 m v s - m v^2 + c_f (l_1 - l_f) + c_r (l_1 + l_r)$$

$$R(s) = m v^2 s + (c_f + c_r) v$$

$$D(s) = l_r l_1 m^2 v^2 s^2 + m v (c_f (l_f^2 + l_1 l_r) + c_r (l_r^2 + l_1 l_r)) s + c_f c_r (l_f + l_r)^2 + m v^2 (c_r l_r - c_f l_f)$$

The robustly decoupled car is described by (11) and the feedback control law (15), which is identical to (19) for $\delta_L \equiv 0$. Substitute (15) into (11) and solve for $\beta_1(s)$ and $r(s)$.

$$\begin{bmatrix} \beta_{1dec}(s) \\ r_{dec}(s) \end{bmatrix} = \frac{1}{D_{dec}(s)} \begin{bmatrix} B_{dec}(s) \\ R_{dec}(s) \end{bmatrix} m_d(s) \quad (21)$$

$$B_{dec}(s) = \ell_1 m v s^2 + (c_r(\ell_1 + \ell_r) - m v^2) s - c_f v$$

$$R_{dec}(s) = s(m v^2 s + (c_f + c_r)v) = sR(s)$$

$$D_{dec}(s) = (\ell_r m v s + c_f(\ell_f + \ell_r))(\ell_1 m v s^2 + c_r(\ell_1 + \ell_r) s + c_r v).$$

For the modified control law with fading integrator substitute (18) into (11) and solve for $\beta_1(s)$ and $r(s)$.

$$\begin{bmatrix} \beta_{1mod}(s) \\ r_{mod}(s) \end{bmatrix} = \frac{1}{D_{mod}(s)} \begin{bmatrix} B_{mod}(s) \\ R_{mod}(s) \end{bmatrix} m_d(s). \quad (22)$$

The terms B_{mod} , R_{mod} and D_{mod} are too long to be printed here.

Steady-state effect of yaw disturbances

For a disturbance unit step input, $m_d(s) = 1/s$, the conventional car has the steady-state response

$$\begin{aligned} \beta_{1st} &= \frac{B(0)}{D(0)} = \frac{m v^2 + c_f(\ell_f - \ell_1) - c_r(\ell_r + \ell_1)}{(c_f \ell_f - c_r \ell_r) m v^2 - c_f c_r(\ell_f + \ell_r)^2} \\ r_{st} &= \frac{R(0)}{D(0)} = \frac{-(c_f + c_r)v}{(c_f \ell_f - c_r \ell_r) m v^2 - c_f c_r(\ell_f + \ell_r)^2}. \end{aligned} \quad (23)$$

The robustly decoupled car has the steady-state response

$$\begin{aligned} \beta_{1st,dec} &= \frac{B_{dec}(0)}{D_{dec}(0)} = \frac{-1}{c_r(\ell_f + \ell_r)} \\ r_{st,dec} &= \frac{R_{dec}(0)}{D_{dec}(0)} = 0 \end{aligned} \quad (24)$$

The yaw rate goes to zero, i.e. the car has a constant yaw angle as a steady-state response to a step yaw disturbance.

The car with fading integrator has the steady-state response

$$\begin{aligned} \beta_{1st,mod} &= \frac{B_{mod}(0)}{D_{mod}(0)} = \beta_{1st} \\ r_{st,mod} &= \frac{R_{mod}(0)}{D_{mod}(0)} = r_{st} \end{aligned} \quad (25)$$

which is the same as the response of the conventional car.

Disturbance attenuation ratios, Frequency limits

For comparison we relate the disturbance frequency responses of the *decoupled car* (resp. *car with fading integrator*) with the disturbance frequency response of the *conventional car*, i. e. we calculate the disturbance attenuation ratio (or sensitivity function).

$$\begin{aligned}\rho_{\beta,dec}(j\omega) &= \frac{B_{dec}(j\omega) D(j\omega)}{D_{dec}(j\omega) B(j\omega)} \\ \rho_{r,dec}(j\omega) &= \frac{R_{dec}(j\omega) D(j\omega)}{D_{dec}(j\omega) R(j\omega)} = \frac{sD(j\omega)}{D_{dec}(j\omega)}.\end{aligned}\quad (26)$$

The influence of the yaw disturbances on β_1 or r is reduced for all frequencies for which $|\rho_{\beta}(j\omega)| < 1$ or $|\rho_r(j\omega)| < 1$ where

$$|\rho_r(j\omega)| = \sqrt{\rho_r(j\omega) \rho_r(-j\omega)}.\quad (27)$$

With (26) it turns out that $|\rho_{r,dec}(j\omega)| < 1$ if and only if

$$a\omega^4 + b\omega^2 + c < 0\quad (28)$$

$$a = 2\ell_f \ell_r \ell_1 m^3 v^4 + [2c_r \ell_r^2 (\ell_1 - \ell_f) - c_f \ell_f (\ell_f (\ell_f + \ell_1) + 2\ell_r \ell_1)] (\ell_1 - \ell_f) m^2 v^2$$

$$b = (c_f \ell_f^2 - 2c_r \ell_r \ell_f) m^2 v^4 + 2c_r (\ell_f + \ell_r)^2 (c_f (\ell_1 - \ell_f) + c_r \ell_r) m v^2 \\ + c_f c_r^2 (\ell_f + \ell_r)^2 (\ell_f - \ell_1) (\ell_f + 2\ell_r + \ell_1)$$

$$c = c_f c_r^2 (\ell_f + \ell_r)^2 v^2.$$

The frequency limit ω_{ℓ} is obtained from the quadratic equation $a\omega^4 + b\omega^2 + c = 0$.

$$\omega_{\ell,dec} = \sqrt{\frac{-b + \sqrt{b^2 - 4ac}}{2a}}.\quad (29)$$

The yaw disturbances are attenuated for frequencies $\omega < \omega_{\ell}$ and amplified for $\omega > \omega_{\ell}$. In Figure 7, (27) (at various velocities) and (29) are shown for specific values of the vehicle parameters (data of a BMW 735i passenger car). Yaw disturbances are attenuated for $\omega < \omega_{\ell} \approx 2\pi \cdot 0.8$ Hz.

Similarly for the *car with fading integrator*

$$\begin{aligned}\rho_{\beta,mod}(j\omega) &= \frac{B_{mod}(j\omega) D(j\omega)}{D_{mod}(j\omega) B(j\omega)} \\ \rho_{r,mod}(j\omega) &= \frac{R_{mod}(j\omega) D(j\omega)}{D_{mod}(j\omega) R(j\omega)}.\end{aligned}\quad (30)$$

The equation corresponding to (28) has the form

$$\omega^2(a^* \omega^4 + b^* \omega^2 + c^*) < 0.\quad (31)$$

The terms a^* , b^* and c^* are too long to be printed here. The absolute value of the disturbance attenuation ratio and the frequency limit of the car with fading integrator are plotted in Figure 8 for the same vehicle data and with the filter bandwidth

$$\omega_0 = 1/\text{sec.} \quad (32)$$

The filter damping coefficient D is scaled with the velocity according to Figure 3 (star markers indicate the considered velocities).

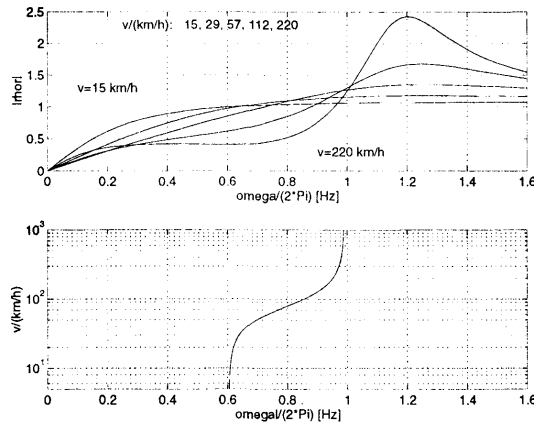


Fig. 7. $|\rho_{r,dec}(\omega)|$ and $\omega_{l,dec}(v)$.

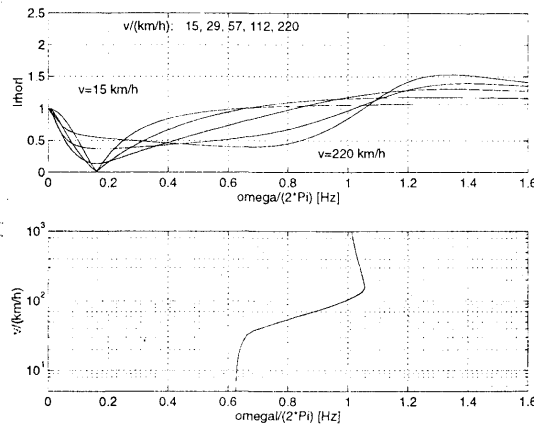


Fig. 8. $|\rho_{r,mod}(\omega)|$ and $\omega_{l,mod}(v)$.

The main difference between the disturbance attenuation ratios of the *decoupled* car and the *car with fading integrator* is to be recognized for low frequencies. For

$\omega \rightarrow 0$, $|\rho_{r,dec}|$ tends to zero which is due to $r_{st,dec} = 0$ (24). However $|\rho_{r,mod}|$ tends to one for $\omega \rightarrow 0$. This shows that the steady-state behaviour with respect to yaw disturbances is the same for the *car with fading integrator* and the *conventional car*. The frequency limits of both disturbance attenuation ratios do not differ essentially. But at high speed, the *car with fading integrator* exhibits less amplification of yaw disturbances beyond the frequency limit.

7. CONCLUSIONS

The *car with fading integrator* can be considered as a compromise between the *conventional car* (which is sensitive to low frequency yaw disturbances) and the *decoupled car* (which exhibits poor yaw damping at higher velocities). In terms of the filter transfer function of the *fading integrator* the *conventional car* corresponds to $\omega_0 \rightarrow \infty$ and the *decoupled car* corresponds to $\omega_0 = 0$. With a bandwidth of $\omega_0 = 1/sec$ and velocity-scaled damping coefficient of the filter a reasonable compromise has been found for acceptable yaw damping and good disturbance attenuation properties at all operating conditions.

Within the minimum driver reaction time of 0.5 seconds, the *car with fading integrator* behaves like the *decoupled car* and then it returns smoothly to the steady-state behaviour of the *conventional car*.

(Received February 14, 1996.)

REFERENCES

-
- [1] J. Ackermann: Robust decoupling of car steering dynamics with arbitrary mass distribution. In: Proc. American Control Conference, Vol. 2, Baltimore 1994, pp. 1964–1968.
 - [2] J. Ackermann and W. Sienel: Robust yaw damping of cars with front and rear wheel steering. IEEE Trans. Control Systems Technology 1 (1993), 1, 15–20.
 - [3] M. Mitschke: Dynamik der Kraftfahrzeuge. Vol. C. Springer, Berlin 1990.
 - [4] J. Ackermann, T. Bunte, H. Jeebe, K. Naab, and W. Sienel: Fahrtsicherheit durch robuste Lenkregelung. Automatisierungstechnik 44 (1996), 5, 219–225.
 - [5] W. Sienel: Design of robust gain scheduling controllers. In: Proc. Euraco Robust and Adaptive Control Tutorial Workshop, Dublin 1994.

Prof. Dr.-Ing. Jürgen Ackermann and Dipl.-Ing. Tilman Bunte, DLR, German Aerospace Research Establishment, Institute for Robotics and System Dynamics, Oberpfaffenhofen, D-82230 Wessling, Germany.